Journal of Computers Vol. 30 No. 4, 2019, pp. 167-175
doi:10.3966/199115992019083004016

Field Source Estimates for Gravity Anomalies by the Wavelet Multi-Scale Transform and Normalized Full Gradient Method

Wei-Hua Liu[1], Gui-Ju Wu[2*]

[1] School of Electric & Electronic Engineering, Wuhan Polytechnic University, Wuhan, China
liuwhsky@126.com

[2] The Key Laboratory of Earthquake Geodesy, Institute of Seismology,
China Earthquake Administration, Wuhan, China
wugjsky@126.com

Received 13 January 2019; Revised 15 January 2019; Accepted 12 March 2019

Abstract. The wavelet multi-scale transform (WMT) was generally used for separate information of field source underground what can show the structure, mine, petroleum and so on very well in horizontal. And the normalized full gradient (NFG) was generally used for downward continuation of the potential field data. In this study, the WMT and NFG method was applied to Bouguer gravity anomalies to obtain the depth of ano-malous body or structure trend. The different regional and local WMT detail shows that the fourth-order ap-proximation are more smoothly than the Bouguer gravity anomalies; there are significant differences in the north-west and south-east portions, the third-order detail are consistent well with faults along horizontal di-rection, and the fifth-order local detail are suitable with the Bouguer gravity anomalies what can show the feature of the Moho surface.Some experiments were performed, for example, the suitable degree of smooth-ing m should be 2 or 3, and the harmonic number is about 30 in the NFG method; The NFG section shows that several Gh transition zones match well with huge faults or structure. Combining the results of the two methods, two faults joint at the depth of about 30km. integrating the advantages of the two methods are easy-to-use and its efficiency can be determined by more applications to field data.

Keywords: gravity inversion, normalized full gradient method, wavelet multi-scale transform

1 Introduction

The gravity field of the earth, as one of the most fundamental physical fields that provides important informa-tion about near surface and inside the earth structure, has various applications in the hydrologic and petroleum exploration [1-2], mineral processing [3], geological mapping [4-5], the revealing of deep structure [6-7], and de-termination of earthquake risk region distributions [8-9]. That is to say, signal source separation and the study of the earth gravity field has important physical significant, especially, the distribution of abnormal body, deep structure and geological structure. How to store, manage, extract and show information has become the focus of scholars.

Many numerical approaches such as glide average method, matched filtering method, discrete wavelet trans-form [10-11], least-squares method [12-13], spectral analysis [14-15], downward continuation [16-17], and Nor-malized full gradient method [18-19] were applied to interpret gravity anomalies. The wavelet multi-scale trans-form (WMT) method that was expressed firstly by Hou et al [20] to interpret the theory for separation of the gravity anomalies, at the same time give the analysis of the gravity data obtained from across China. WMT is one of the most powerful methods to determine the underground

* Corresponding Author

structures of gravity data in different depth on the transverse. The main reason to use the WMT is horizontal continuation maps. This technique has been developed to decompose the gravity bouguer anomalies and characterize their feature of the different depth sources in the horizontal direction. But the WMT method is not good at showing the field source details in vertical of the grav-ity anomalies. In the above methods, the normalized full gradient (NFG) can be applied to identify the structural trend, and the trend of the abnormal bodies in vertical, using the method can get downward continuation maps. And the analytical downward continuation is an effective method to estimate the field closer to the source, therefore, its results in a better resolution of the distribution of the underground field source. Although the NFG is one of the best approaches for locating the underground source from gravity anomalies, its resolution in horizontal is not better to show the details of the underground matters.

In order to understand the features of underground structures and field source, the paper combined the advan-tages of the WMT and NFG in horizontal and vertical to research the underground characteristics. Based on acquiring acceptable results of using the WMT and NFG method, real and model data of gravity data in the Jilan-tai rift zone and its adjacent region is interpreted where is located in the west Ordos of China.

2 The Theory of Field Source Separation

2.1 The Wavelet Multi-scale Transform

The processing of the WMT includes wavelet decomposition and its reconstruction of the gravity data, and it is based on the theory of Mallat [21]. The wavelet theory is defined by scale function $\phi(x)$ and wavelet function $\psi(x)$. Assuming $V_j^2=V_j \otimes V_j$, then the 2-dimensional (2-D) multi-scale function will be composed by $\{V_j^2\}_{j\in z}$, the scale function is as following:

$$\phi(x,y)=\phi(x)\cdot\phi(y) \tag{1}$$

The wavelet function is

$$\psi^h(x,y)=\psi(x)\cdot\phi(y) \tag{2}$$

$$\psi^v(x,y)=\phi(x)\cdot\psi(y) \tag{3}$$

$$\psi^d(x,y)=\psi(x)\cdot\psi(y) \tag{4}$$

Setting the 2-D function $f(x, y)$ is multi-scale function, that's to say $f(x, y)\in\{V_j^2\}_{j\in z}$, if $A_jf(x)$ represents the low-frequency detail information in V_j^2, and $D_j^h f(x)$, $D_j^v f(x)$ and $D_j^d f(x)$ are the horizontal, vertical and diagonal high-frequencies detail information respectively in V_j^2, then,

$$A_j f(x,y)=A_{j+1}f(x,y)+D_{j+1}^h f(x,y)+D_{j+1}^v f(x,y)+D_{j+1}^d f(x,y) \tag{5}$$

Where

$$\begin{cases} A_{j+1}f(x,y)=\sum\limits_{m_1,m_2\in Z} S_{m_1,m_2}^{j+1}\phi_{j,m_1,m_2} \\ D_{j+1}^T f(x,y)=\sum\limits_{m_1,m_2\in Z} d_{m_1,m_2}^{T,j+1}\psi_{j,m_1,m_2}^T \qquad (T=h,v,d) \end{cases} \tag{6}$$

And

$$S_{m_1,m_2}^{j+1}=\sum_{k_1,k_2\in Z} h_{k_1-2m_1}h_{k_2-2m_2}s_{j,m_1,m_2} \tag{7}$$

$$d_{m_1,m_2}^{h,j+1}=\sum_{k_1,k_2\in Z} h_{k_1-2m_1}g_{k_2-2m_2}s_{j,m_1,m_2} \tag{8}$$

$$d_{m_1,m_2}^{v,j+1} = \sum_{k_1,k_2 \in Z} g_{k_1-2m_1} h_{k_2-2m_2} s_{j,m_1,m_2} \tag{9}$$

$$d_{m_1,m_2}^{d,j+1} = \sum_{k_1,k_2 \in Z} g_{k_1-2m_1} g_{k_2-2m_2} s_{j,m_1,m_2} \tag{10}$$

In order to get the gravity anomalies in different depth, now we set the gravity anomalies function is $\Delta g(x, y)$, for the 2-D gravity field anomalies its wavelet multi-scale transform is as following

$$\Delta g(x,y) = A_0 f(x,y) = A_4 f(x,y) + \sum_{j=1}^{4} (D_j^h f(x,y) + D_j^v f(x,y) + D_j^d f(x,y)) \tag{11}$$

As well, assuming the gravity date with regular grids is the coefficient $\{s^0\}$of the scale function V_0^2, then in terms of the equations (7)-(10) we can calculate the coefficient {dh, j}, {dv, j} and{dd, j} of wavelet function, and the coefficient {sj}of scale function. Taking the fourth order of 2-D wavelet transform for example, the shorthand calculating function is $\Delta g(x)$

$$\Delta g(x) = A_4 G + D_4 G + D_3 G + D_2 G + D_1 G \tag{12}$$

Where A_4G is the fourth order approximation of the WMT, which is the low-frequency detail information, D_jG is the jth order high-frequency detail part of the WMT and the value of j is integer 1 to 4. And the calculating process will be continued until the desired results are achieved, at this point the approximation of WMT and details have the similar resolution as A_j at the jth order. Finally, the Wavelet multi-scale transform is applied to gravity data; we get the results of gravity anomalies in different depth.

2.2 The NFG Method

The NFG operator $G^h(x, z)$ constitutes the basic concept of the NFG method and is defined in two dimensions as:

$$G^h(x,z) = \frac{G(x,z)}{\overline{G}(x,z)} = \frac{\sqrt{V_{xz}{}^2(x,z) + V_{zz}{}^2(x,z)}}{\frac{1}{K+1}\sum_{i=0}^{N}\sqrt{V_{xz}{}^2(x,z) + V_{zz}{}^2(x,z)}} \tag{13}$$

where, $G(x, z)$ is the NFG on the cross-section x-z at point (x, z); $\overline{G}(x, z)$ is the average value of the NFG of K+1 observation points at the z depth; $V_{xz}(x, z)$ and $V_{zz}(x, z)$ are the first vertical derivative and the first horizontal derivative of gravity anomalies at the point (x, z) along the x axis; K is the number of observation points; the equation 1 shows that $G^h(x, z)$ is a dimensionless ratio, it is divided by the average value of $G(x, z)$; and then the NFG $G^h(x, z)$ of each point will be calculated at certain depth intervals.

When the value of gravity anomalies is zero on both ends of the measuring line, the Sine series converges is faster than the Cosine series, therefore the Sine series were chosen to represent the gravity anomalies Δg; and each Δg should minus linear term $a+bx$, where a is the value of the starting point $\Delta g(0, 0)$ of the measuring line, b is the slope of the line, it will be calculated as:

$$b = [\Delta g(0,0) - \Delta g(0,L)] / L \tag{14}$$

Where Δg(0, L) is the value of the end point and L is the length of the line, then we can get a formula for the gravity Fourier series, then we can get a formula for the gravity Fourier series:

$$\Delta g(x,z) = \sum_{1}^{N} B_n \sin\frac{\pi n x}{L} e^{\frac{\pi n x}{L}} \tag{15}$$

N is harmonic number, $e^{\pi nx/L}$ is downward factor, and B_n is harmonic coefficient, $V_{xz}(x, z)$ and $V_{zz}(x, z)$ can be get by taking the derivative of the formula (15), as following:

$$V_{xz}(x,z) = \frac{\pi}{L}\sum_{1}^{M} nB_n \cos\frac{\pi n x}{L} e^{\frac{\pi n x}{L}} \tag{16}$$

$$V_{zz}(x,z)=\frac{\pi}{L}\sum_{1}^{M}nB_n\sin\frac{\pi nx}{L}e^{\frac{\pi nx}{L}} \tag{17}$$

According to the above formulas, we can assume L is made up of the measurement points K+1with a distance Δx between them, then

$$x=j\Delta x(j=0,1,2,\cdots,N) \tag{18}$$

$$L=K\Delta x \tag{19}$$

Finally, the B_n can be show as following:

$$B_n=\frac{2}{K}\sum_{j}^{K}\Delta g(j\Delta x)\sin\frac{\pi nj}{K} \tag{20}$$

In order to resolve false exceptions of $G^h(x, z)$, the B_n multiplies by a smoothing factor q_m to enhance its stability,

$$q_m=\left(\frac{\sin\pi n/N}{\pi n/N}\right)^m \tag{21}$$

Where, N is the sum of harmonic number, m is the degree of smoothing, and q_m can eliminate high frequency noise resulting from downward continuation, its value range is from 1 to 0, as n increasing, the smoothing function of q_m become more strong. And the behavior of the q_m equation is shown in Fig. 1. Generally speaking, m takes 2 or 3 is better, and it is assumed m equal to 2 in this study. We can get the $V_{xz}(x, z)$ and $V_{zz}(x, z)$ equations

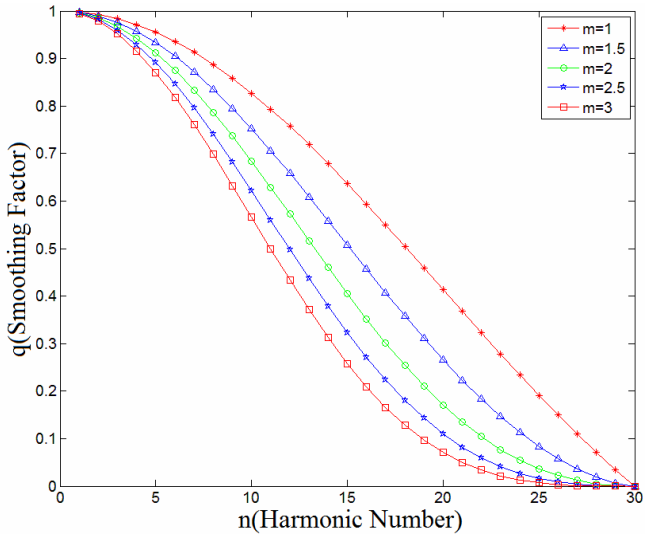

Fig. 1. The behavior of q_m function

$$V_{xz}(x,z)=\frac{\pi}{L}\sum_{1}^{N}nB_n\cos\frac{\pi nx}{L}e^{\frac{\pi nx}{L}}\left(\frac{\sin(\pi n/N)}{(\pi n/N)}\right)^2 \tag{22}$$

$$V_{zz}(x,z)=\frac{\pi}{L}\sum_{1}^{N}nB_n\sin\frac{\pi nx}{L}e^{\frac{\pi nx}{L}}\left(\frac{\sin(\pi n/N)}{(\pi n/N)}\right)^2 \tag{23}$$

The Equation (22) and (23) are substituted into equation (13), the normalized full gradient (NFG) of gravity is calculated. The key influencer of the NFG is the harmonic number. We can select suitable N in terms of the length of the line, if the length of the line is short, N is small, and otherwise, N is big. The

method is useful for detecting the distribution characteristic of underground bodies.

3 Application of the WMT and NFG

The research data is shown in Fig. 2, where the blue solid dot are cities, the blue line is the gravity profile. the red solid line are faults, F1:Yabulaishan fault, F2: Bayanwulashan fault, F3:Wuyuan-Hangjinhouqi fault, F4: Dengkou-Benjing fault, F5: Zhengyiguan fault, F6: Helandonglu fault, F7: Yinchuan concealed fault, F8: Yellow River fault, F9: the northern rim of Ordos fault. The data is the region bouguer gravity anomaly. It is compiled in terms of the EGM2008 model gravity data, 1:1 million Chinese bouguer gravity anomalies and airborne gravity data, and it reflects the whole substance distribution what is formed by tectonic deformation for a long time between the Alxa and Ordos block. On the whole, the spreading of the regional gravity anomaly is from low-high-low. There is a low anomaly zone between F2 and F6 where it passes the Jilantai rift zone. And between F4 and F8, there is a local high gravity anomaly, it is mainly located in Pingluo area, the range of anomaly value is from -151mGal to -127mGal. The directions of faults in the research area are mainly consistent with the strike of the contour of the bouguer gravity, for example, F2, F6, F7 and F8. In this paper, we use the WMT method to calculate the gravity anomalies in different order; then the NFG method is used to calculate what is to shown the distribution of the depth field source in vertical.

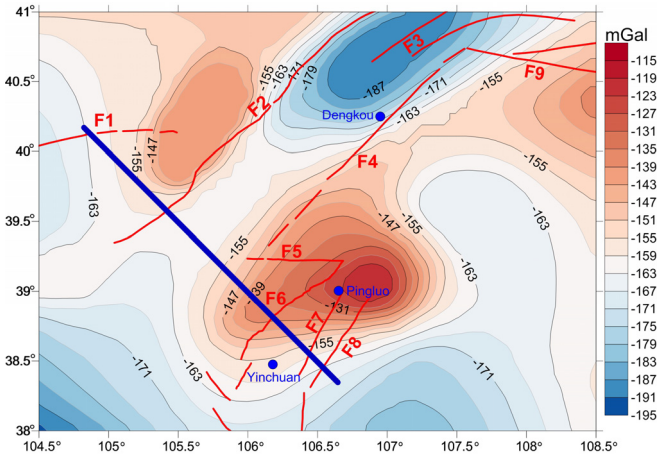

Fig. 2. The distribution of gravity anomalies. The red solid line is fault; the blue solid dot is city, the blue line is the gravity profile. F1: Yabulaishan fault, F2: Bayanwulashan fault, F3: Wuyuan-Hangjinhouqi fault, F4: Dengkou-Benjing fault, F5: Zhengyiguan fault, F6: Helandonglu fault, F7: Yinchuan concealed fault, F8: Yellow River fault, F9: the northern rim of Ordos fault

3.1 The Result of Wavelet Multi-scale Decomposition

Because of the data in the research area, the resolution is about 10km. The first-order and the second-order 2-D WMT details are abandoned. The Fig. 3 shows that the second-order 2-D WMT decomposition of Bouguer gravity anomalies separates the regional and local anomalies. In the paper, we selects the fourth-order 2-D WMT approximation as the regional anomalies (shown in Fig. 3(a)) comparing with the other order 2-D WMT, we can find that the map of regional Bouguer gravity anomalies reveals the whole structure distribution more smoothly than the Bouguer gravity anomalies(shown in Fig. 2). The low- high or high-low transformation belts are mainly along the faults F2 and F4 what is the history depth and huge fault and its with anomalies between -195mGal and -120mGal, and between of the two faults is the Jilantai rift zone, where is composed by low Bouguer gravity anomalies. The results of the different-order WMT detail can exhibits the distribution of depth structure in horizontal direction.

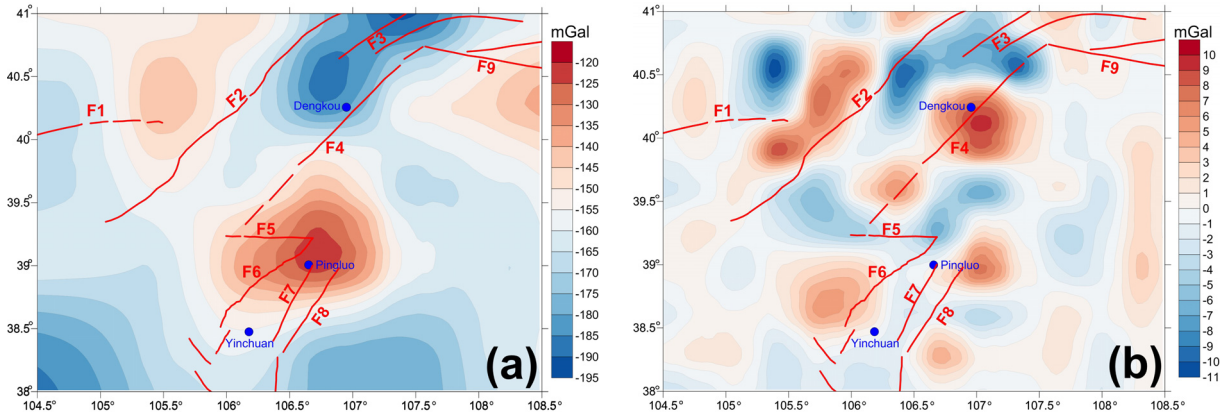

Fig. 3. The regional and local gravity anomalies of the west Ordos are separated by the WMT method. Fig. 3(a) is the regional anomalies the fourth-order WMT approximation, and Fig. 3(b) is the local anomalies what is the results of removing the approximation from the Bouguer gravity anomalies shown in Fig. 2

The Fig. 4 reveals the subsurface structure distribution in the west Ordos from the upper crust to the lower as far as to the Moho surface. The high local gravity anomalies are very scattered in the third and fourth order WMT detail, that is to say, it mainly show the upper crust lower density bodies especially in Fig. 4(a), the low-high transformation belts fit poor with the faults in the region. In Fig. 4(b), F1, F2, F5, F6, F7, F8 are mainly located in the transformation belts. And as the order increasing, we can find that the huge faults are fit very well with the transformation belt, as F2 and F4. But the sixth-order WMT details are large gap compare with the others order details, therefore, all results after sixth-order are abandoned in the study. All in all, the results of 2-D WMT details can just show the distribution of the underground field source in x, y direction.

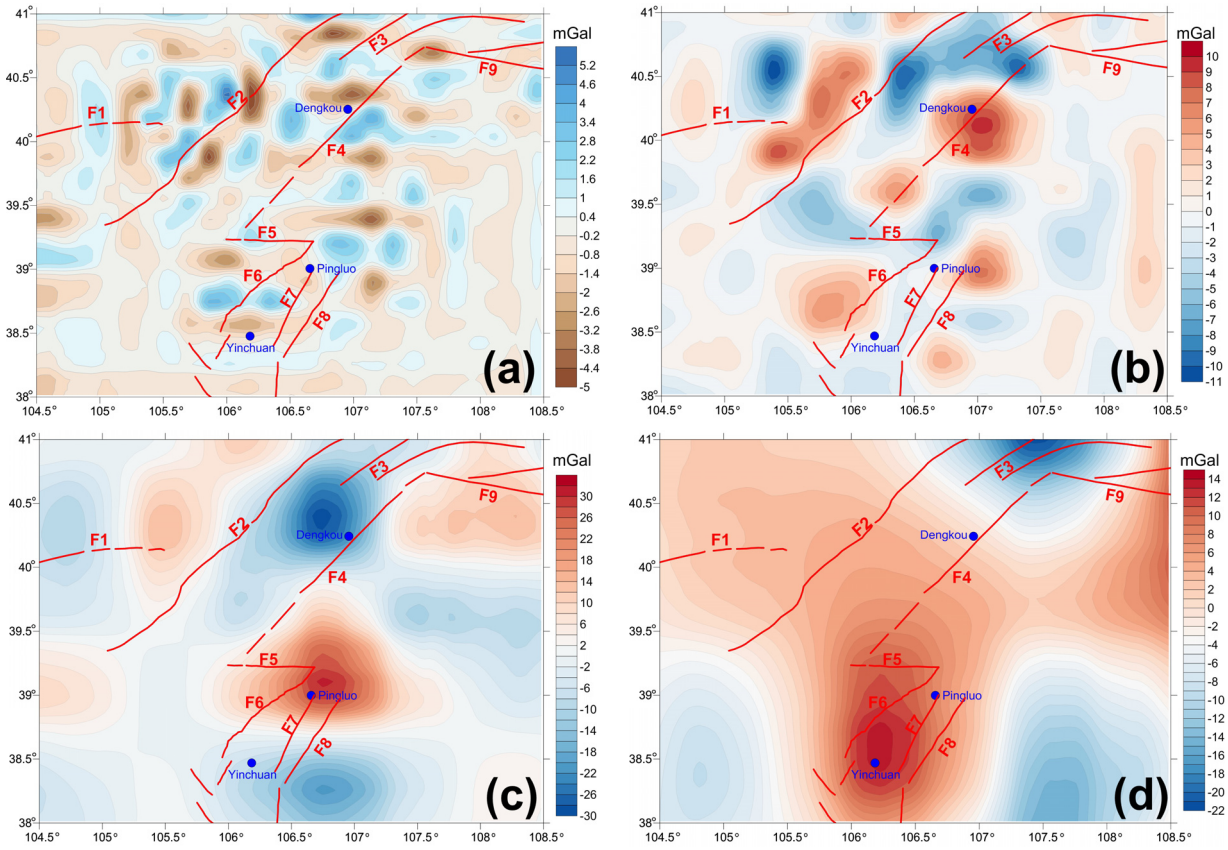

Fig. 4. The Maps showing the WMT details from third-order to sixth-order of the Bouguer gravity anomalies for the west Ordos region. Fig. 3(a) third-order details, Fig. 3(b) fourth-order details, Fig. 3(c) fifth-order details, Fig. 3(d)sixth-order details

3.2 The Result of NFG

In order to show the efficiency of the NFG method in estimating the depths of the gravity anomalies, the method is applied to a gravity profile data (shown in Fig. 2). The theoretical anomalies over the region are located at the low-high transformation belt in the profiles. In this study, a NFG section is calculated using different harmonic intervals in order to get the suitable harmonic limits. Because the profile is about 260km, therefore the value of N can't be too big or too small. If the N is set less than 20, we will get same false anomalies, the N is set greater than 40, and the results will be too smoothing to cover up the real anomalies.

The profile gravity anomaly is a linear interpolation with 1km, the harmonic numbers are 20 (Fig. 5(a)) and 30 (Fig. 5(b)), the plane on which the downward continuation is 1km, and we obtain the image of the NFG along the profile shown in Fig. 5. The main characteristics of the gravity profile are that the distribution of G^h is complex in the upper crust from west to east along the profile and there are several transition zones of high and low G^h, located at about -10km, -85km, -30km, -5km, 50km, 70km, and 110km.The value of the G^h change is caused by the difference of the subsurface densities. It is observed from the NFG sections that several faults response profile match well with transition zones of the NFG depth contours. For instance, F1, F2, and F7 faults are consistent with the NFG gradient zone in Fig. 5; but in Fig. 5(a) there are more the transition zones than in Fig. 5(b). Because of the gravity profile is too long, the harmonic number is smaller, the false anomalies will be more; when the harmonic number N is 30, the transition zones match well with the faults.

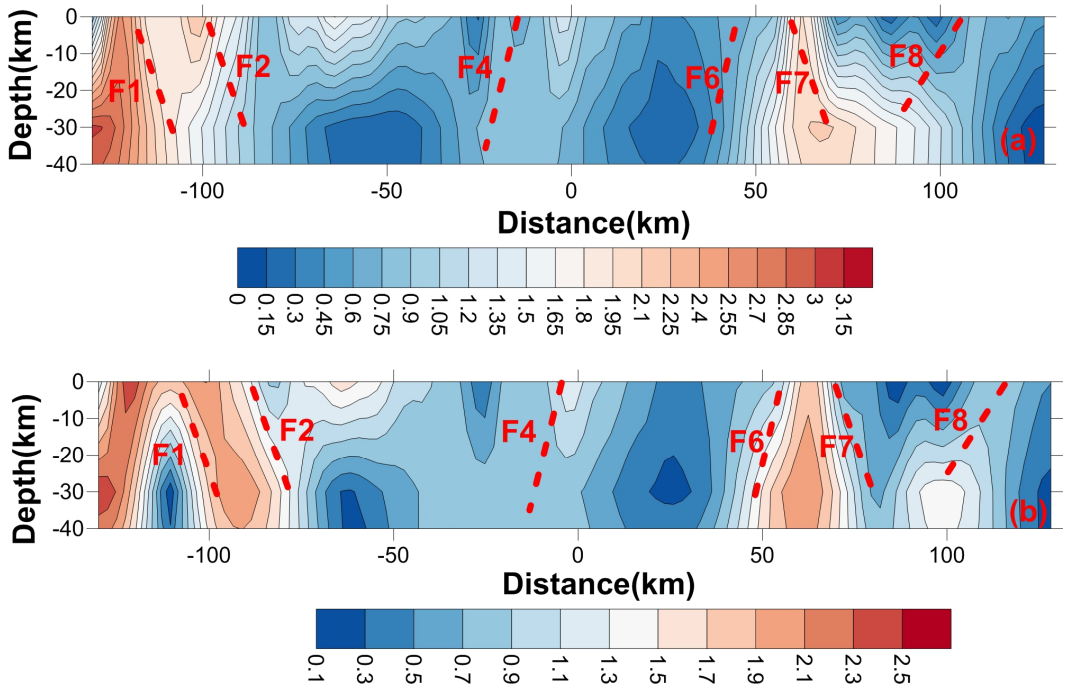

Fig. 5. The depth estimates image of the NFG of the gravity profile at N =20 and N=*30*.

4 Discuss and Conclusions

The WMT provides an effective method for interpreting the underground field source based on gravity data. From analyzing regional and local anomaly of the upper crust structure and the surrounding regions shows that the Fourth-order WMT regional detail is closely correlated with the tectonic characteristics in the west Ordos. And there are significant differences in the north-west and south-east portions, from the local anomalies (Fig. 4), the third-order detail are consistent well with faults along horizontal direction, and the fifth-order local detail are suitable with the Bouguer gravity anomalies what can show the feature of the Moho surface.

The NFG method of obtaining depth estimates appears to be a practical tool to estimate the faults and mines depth values from gravity anomalies., The advantage of the NFG method is that, it does not

depend on any other geophysical results, and the results match well with anomaly bodies, and therefore it is possible to extend the downward continuation to the depths below the anomaly field source and easy to code in computer and requires only a small calculating time. The main characteristic of the NFG sections of gravity anomalies is that it contains several transition zones where match well with huge faults or structure. However, the NFG method can just show anomalies along profile, that's to say, the method can just exhibits well in vertical.

Combing the result of NFG method and WMT, it can be observed that the F7 and F8 joint at the depth of about 30km. The two faults are all at the transition zone in different order of the WMT detail, and the NFG section the value of the G^h change is from low to high at N=30, in other words there is a low density anomaly bodies. The combining the advantages of the two methods are easy-to-use and its efficiency can be determined by more applications to field data.

Acknowledgements

This work is supported by the National Natural Science Foundation of China (41704135)

References

[1] H.L. Zeng, X.M. Li, C.L. Yao, X.H. Meng, H. Lou, Z.N. Guan, Z.P. Li, The modified normalized full gradient of gravity anomalies and its application to Shengli oil field, East China, Petroleum Exploration and Development 26(6)(1999) 1-6.

[2] R.N. Bohidar, J.P. Sullivan, J.F. Hermance, Delineating depth to bedrock beneath shallow unconfined aquifers: a gravity transect across the Palmer River Basin, Ground Water 39(5)(2001) 729-736.

[3] J.G. Damaceno, de D.L. Castro, S.N. Valcácio, Magnetic and gravity modeling of a Paleogene diabase plug in Northeast Brazil, Journal of Applied Geophysics 136(1)(2017) 219-230.

[4] A. Gabas, A. Macau, B. Benjumea, Combination of geophysical methods to support urban geological mapping, Surveys in Geophysics 35(4)(2014) 983-1002.

[5] S. Brooke-Barnett, G. Rosenbaum, Structure of the Texas Orocline beneath the sedimentary cover (southeast Queensland, Australia), Australian Journal of Earth Sciences 62(4)(2015) 425-445.

[6] Y. Wei, Z.J. Yang, The application of combined gravity and seismic data formation separation for revealing deep structure, Applied Geophysics 3(4)(2006) 255-259.

[7] D.J. Holden, N.J. Archibald, F. Boschetti, Inferring geological structures using wavelet-based multiscale edge analysis and forward models, Exploration Geophysics 31(4)(2000) 617-621.

[8] J.T. Kuo, Y.F. Sun, Modeling gravity variations caused by dilatancies, Tectonophysics 227(1)(1993) 127-143.

[9] C.Y. Shen, H. Li, S.A. Sun, S.M. Liu, S.B. Xuan, H.B. Tan, Dynamic variations of gravity and the preparation process of the WenChuan Ms8.0 earthquake, Chinese Journal of Geophysics 52(10)(2009) 2547-2557.

[10] H. Lou, C.Y. Wang, Wavelet analysis and interpretation of gravity data in Sichuan-Yunnan region, China. Acta Seismol Sin 18(5)(2005) 552-561.

[11] S.B. Xuan, C.Y. Shen, H. Li, H.B. Tan, Structural interpretation of the Chuan-Dian block and surrounding regions using discrete wavelet transform, International Journal of Earth Sciences 105(5)(2016) 1591-1602.

[12] J. Asfahani, M. Tlas, A nonlinear programming technique for the interpretation of self-potential anomalies, pure and applied geophysics 159(6)(2002) 1333-1343.

[13] J. Asfahani, M. Tlas, A constrained nonlinear inversion approach to quantitative interpretation of selfpotential anomalies caused by cylinders, spheres and sheet-like structures, Pure and Applied Geophysics 162(3)(2005) 609-624.

[14] N. Sundararajan, Y. Srinivas, A modified Hilbert transform and its application to self-potential interpretation, Journal of Applied Geophysics 36(2)(1996) 137-143.

[15] W.C. Yang, Y.Y. Sun, Z.Z. Hou, C.Q. Yu, An multi-scale scratch analysis method for quantitative interpretation of regional gravity fields, Chinese Journal of Geophysics 58(2)(2015) 520-531.

[16] M. Fedi, G. Florio, A stable downward continuation by using the ISVD method, Geophysical Journal International, 151(1)(2002) 146-156.

[17] X.J. Li, Z.L. Wang, A study on gravity field downward continuation using the regularized equivalent-layer method, Chinese Journal of Geophysics 61(7)(2018) 3028-3036.

[18] M. Abedi, M.K. Hafizi, G.H. Norouzi, 2D interpretation of self-potential data using normalized full gradient, a case study: galena deposit, Bollettino di Geofisica Teorica ed Applicata 53(2)(2012) 213-230.

[19] G.J. Wu, C.Y. Shen, H.B. Tan, G.L. Yang, Tectonic implication of images of bouguer gravity anomaly and its normalized total gradient in 2015 Alashanzuoqi Ms5.8 Area, Journal of Geodesy and Geodynamics 35(6)(2015) 936-940.

[20] W.C. Yang, Z.Z. Hou, Wavelet transform and Multi-scale analysis on gravity anomalies of China, Acta Geophysica Sinica 40(1)(1997) 85-95.

[21] S. Mallat, A theory for multiresolution signal decomposition: the wavelet representation, IEEE Transactions on Pattern Analysis and Machine Intelligence 11(7)(1989) 674-693.